Journal of Biomechanics 58 (2017) 203–211

Contents lists available at ScienceDirect

Journal of Biomechanics

journal homepage: www.elsevier.com/locate/jbiomech
www.JBiomech.com

Dynamic head-neck stabilization and modulation with perturbation bandwidth investigated using a multisegment neuromuscular model

Riender Happee [a,*,1], Edo de Bruijn [a,1], Patrick A. Forbes [a,c], Frans C.T. van der Helm [a,b]

[a] Department of Biomechanical Engineering, Delft University of Technology, Delft, The Netherlands
[b] Laboratory of Biomechanical Engineering, University of Twente, Enschede, The Netherlands
[c] Department of Neuroscience, Erasmus Medical Centre, Rotterdam, The Netherlands

ARTICLE INFO

Article history:
Accepted 8 May 2017

Keywords:
Postural control
Musculoskeletal model
Neck
Feedback
Vestibular
VCR
CCR
Co-contraction

ABSTRACT

The human head-neck system requires continuous stabilization in the presence of gravity and trunk motion. We investigated contributions of the vestibulocollic reflex (VCR), the cervicocollic reflex (CCR), and neck muscle co-contraction to head-in-space and head-on-trunk stabilization, and investigated modulation of the stabilization strategy with the frequency content of trunk perturbations and the presence of visual feedback.

We developed a multisegment cervical spine model where reflex gains (VCR and CCR) and neck muscle co-contraction were estimated by fitting the model to the response of young healthy subjects, seated and exposed to anterior-posterior trunk motion, with frequency content from 0.3 up to 1, 2, 4 and 8 Hz, with and without visual feedback.

The VCR contributed to head-in-space stabilization with a strong reduction of head rotation (<8 Hz) and a moderate reduction of head translation (>1 Hz). The CCR contributed to head-on-trunk stabilization with a reduction of head rotation and head translation relative to the trunk (<2 Hz). The CCR also proved essential to stabilize the individual intervertebral joints and prevent neck buckling. Co-contraction was estimated to be of minor relevance. Control strategies employed during low bandwidth perturbations most effectively reduced head rotation and head relative displacement up to 3 Hz while control strategies employed during high bandwidth perturbations reduced head global translation between 1 and 4 Hz. This indicates a shift from minimizing head-on-trunk rotation and translation during low bandwidth perturbations to minimizing head-in-space translation during high bandwidth perturbations. Presence of visual feedback had limited effects suggesting increased usage of vestibular feedback.

1. Introduction

The human head-neck system is a complex and highly flexible biomechanical structure, requiring continuous active stabilization in the presence of gravity. Coordinated feedback control of neck muscle segments is needed to position and stabilize the head in space, and to stabilize the individual neck joints in the presence of trunk motion and other perturbations. These are partly conflicting control objectives. In the presence of dynamic trunk motion, for example while walking or riding in a vehicle, it may be beneficial to minimize head rotation and translation to improve vision and comfort. This can be achieved with a so called head-in-space control strategy using vestibular and visual feedback. In contrast, humans may employ a head-on-trunk control strategy using muscle spindle feedback and co-contraction of antagonist muscles to stiffen the neck and stabilize individual neck joints to prevent neck buckling (collapse) in the presence of gravity.

Experimental studies have demonstrated that muscle spindle and vestibular afferent information contribute to head-neck stabilization through the cervicocollic reflex (CCR) and the vestibulocollic reflex (VCR), respectively (Keshner et al., 1999; Keshner, 2009; Goldberg and Cullen, 2011; Cullen, 2012; Forbes et al., 2013a). This paper investigates the role of the VCR, CCR and co-contraction using an advanced neuromuscular model. An early model captured human response data to sagittal plane torso perturbations with a two-pivot head-neck model (Peng, 1996). The model attributed substantial VCR and CCR contributions to head pitch rotation control, but head translation, which is commonly assumed to be also under VCR and CCR control was not reported. Thus our study aims

* Corresponding author at: Faculty of Mechanical, Maritime and Materials Engineering (3mE), Delft University of Technology, The Netherlands.
E-mail address: R.Happee@tudelft.nl (R. Happee).
[1] Both authors contributed equally.

http://dx.doi.org/10.1016/j.jbiomech.2017.05.005
0021-9290/

to corroborate previous findings on head rotation control and extend them to head translation to support hypothesis 1: *The VCR contributes to head-in-space stabilization and substantially reduces head rotation and translation in space, while the CCR contributes to head-on-trunk stabilization and substantially reduces head rotation and translation relative to the trunk.*

Local neck deformation like S-shaped bending cannot be (accurately) sensed by the vestibular organ, since it encodes head motion in gravito-inertial coordinates. As a result, muscle length and velocity feedback are expected to be essential for the stabilization of the individual neck joints and to prevent neck buckling (collapse) in the presence of gravity. We therefore define hypothesis 2: *The CCR stabilizes the intervertebral joints and prevents neck buckling.*

Experimental and modelling studies on the extremities and lumbar spine have shown substantial contributions of muscle co-contraction, where simultaneous activation of antagonist muscles creates an "intrinsic resistance" which can be of a similar magnitude as the "reflexive resistance" (Kearney et al., 1997; Mirbagheri et al., 2000; de Vlugt et al., 2006; van Drunen et al., 2013). Keshner (2000) reported effects of neck muscle co-contraction when young (20–40 year) subjects were asked to stiffen their necks, but this effect was absent when subjects performed mental arithmetic or relax tasks. This motivates hypothesis 3: *Co-contraction can contribute to head-on-trunk stabilization, but this contribution will be minor in natural stabilization conditions.*

Experimental studies have shown the ability of the central nervous system (CNS) to modulate neck afferent feedback in response to changing external environments (Goldberg and Peterson, 1986; Gillies et al., 1998; Keshner et al., 1999; Fard et al., 2004; Liang and Chiang, 2008; Reynolds et al., 2008). We demonstrated modulation of neck afferent feedback with the frequency bandwidth of anterior-posterior trunk perturbations (Forbes et al., 2013b), with modest effects of the presence of vision. We tentatively associated this modulation with the attenuation of oscillations, and with a shift from head-on-trunk to head-in-space to stabilization. In line with the experimental data (Forbes et al., 2013b) we define hypothesis 4: *The presence of higher frequencies in the perturbations will induce a shift from head-on-trunk to head-in-space stabilization.* The head-in-space strategy will minimize the seat to head transmission, which can be beneficial for motion comfort (Paddan and Griffin, 1998).

To evaluate the above hypotheses, we developed an advanced neuromuscular model of the human head-neck system. Contributions of VCR, CCR and co-contraction were investigated fitting the model to responses of young healthy subjects exposed to anterior-posterior trunk perturbations with varying bandwidth, during eyes closed and eyes open conditions (Forbes et al., 2013b).

2. Methods

Neuromuscular neck models presented in the literature range from 1-pivot models (Peng, 1996; Peng et al., 1997; Peng et al., 1999; Fard et al., 2003; Rahmatalla and Liu, 2012; Wang and Rahmatalla, 2013) to detailed multisegment models (van Ee et al., 2000; Wittek et al., 2000; Yoganandan et al., 2002; Chancey et al., 2003; Stemper et al., 2004; Brolin et al., 2008; Hedenstierna, 2008; Almeida et al., 2009; Meijer et al., 2013; Östh et al., 2016). To study stabilization of the individual intervertebral joints, a multisegment model is needed. Chancey et al. (2003) presented a multisegment neck model and used optimization to generate balanced activations of 23 muscle pairs representing relaxed and maximally tensed initial states, minimising intervertebral motion while exposing the model to gravity for 100 ms. However we found no proof that any existing multisegment neck model stabilizes the individual joints in the presence of gravity with prolonged dynamic perturbations. The VCR and CCR can separately control head rotation and translation, but we are not aware of any model including such separate feedback loops.

In order to address the above limitations, a three-dimensional (3D) multisegment nonlinear neck model (de Jager, 1996; van der Horst, 2002; de Bruijn et al., 2015) was extended with a new control model (Fig. 1).

2.1. Biomechanical head-neck model

The model contains nine rigid bodies representing the head, seven cervical vertebrae (C1–C7), and the first thoracic vertebra (T1). The head mass is 4.69 kg and the total neck mass is 1.63 kg (van der Horst, 2002). The 8 intervertebral joints allow 3D rotational and translational motion, resulting in a total of 48 degrees of freedom (DOF). Centers of rotation are not imposed and joint motion is governed by non-linear models of the passive structures. Intervertebral discs, ligaments

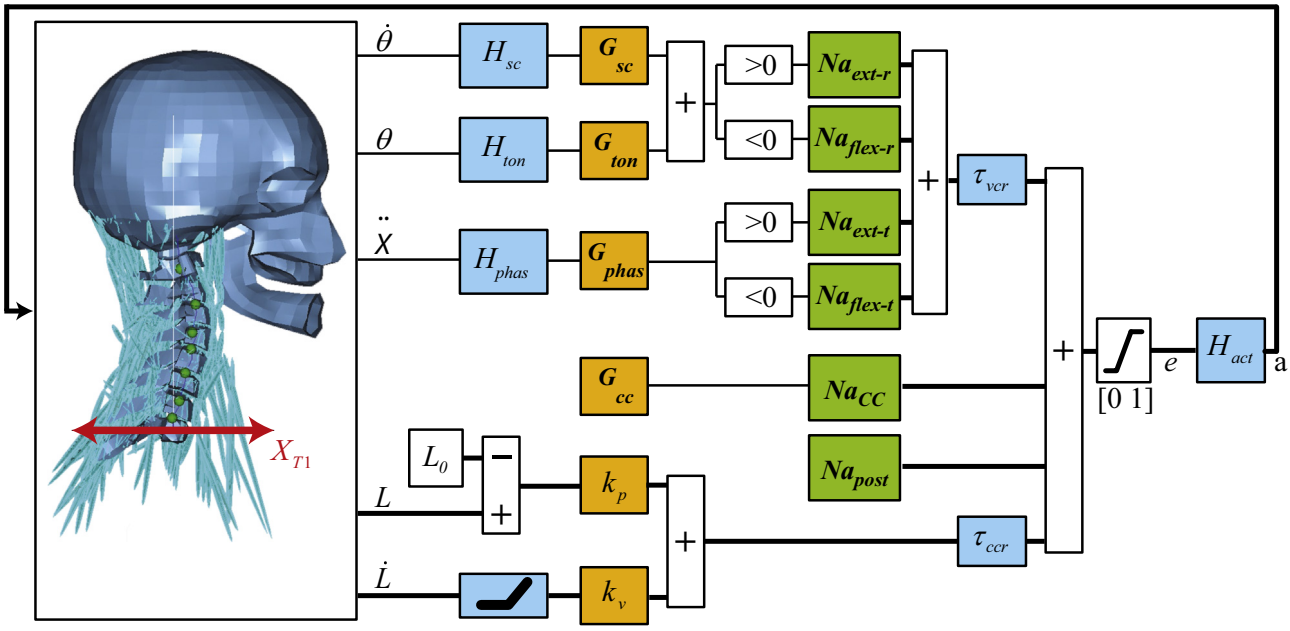

Fig. 1. Neural control model. Blue blocks contain sensory and muscle activation dynamics and delays, orange blocks contain the feedback sensitivity (gain) and co-contraction parameters. Green blocks are muscle synergy vectors converting scalar control signals to an appropriate activation of multiple muscle segments for flexion ($Na_{flex\text{-}r}$ for rotation, $Na_{flex\text{-}t}$ for translation), extension ($Na_{ext\text{-}r}$ for rotation, $Na_{ext\text{-}t}$ for translation), co-contraction (Na_{cc}) and postural activity counteracting gravity (Na_{post}). The VCR provides feedback of head angular velocity $\dot{\theta}$, angle θ, and acceleration $\ddot{X}$ with sensor dynamics H_{sc}, H_{ton}, H_{phas}, and feedback sensitivity parameters G_{sc}, G_{ton}, G_{phas}. The CCR provides feedback of muscle contractile element (CE) length L with sensitivity parameter k_p and velocity $\dot{L}$ with sensitivity parameter k_v where muscle CE reference length L_0 represents the desired posture. Neural pathway delays are defined for VCR (τ_{vcr}) and CCR (τ_{ccr}). H_{act} captures muscular activation dynamics transforming neural excitation (e) into muscle active state (a). X_{T1} is the applied mechanical perturbation being translation of the base of the neck. Thick lines indicate multiple signals for all 258 muscle segments.

and facet joints were captured with nonlinear models using biomechanical literature (Pintar, 1986; Yoganandan et al., 1998; Panjabi et al., 2001; van der Horst, 2002). Muscles (34 muscles, totalling 129 elements per body side) were implemented as line elements based on dissection of a single specimen (Borst et al., 2011). Intermediate 'via points' connecting muscles to adjacent vertebrae were implemented to ensure the muscles took on a curved path during head-neck displacement. The non-linear Hill type muscle dynamics are described in the Appendix and further information on the biomechanical model as well as its isometric and passive validation can be found in de Bruijn et al., (2015). Gravity was simulated as a 9.81 m/s^2 gravitational field acting on the skull and the vertebrae.

2.2. Neural control

The neural controller was implemented to stabilize the head-neck model in the anterior-posterior direction in order to simulate the experimental conditions described by Forbes et al. (2013b) (Fig. 1). The activation of muscle segments was regulated by vestibular (VCR) and muscle (CCR) afferent feedback as well as neck muscle co-contraction. The VCR was comprised of three sensory feedback pathways: 1) canal feedback (H_{sc}, G_{sc}) evoked by head angular (pitch) velocity ($\dot{\theta}$), 2) otolith tonic feedback representing graviception (H_{ton}, G_{ton}) evoked by head pitch angle (θ), and 3) otolith phasic feedback (H_{phas}, G_{phas}) evoked by global head acceleration ($\ddot{X}$) in the anterior-posterior direction. In these loops, H captures the sensor dynamics while G is the feedback sensitivity parameter. The CCR was modelled using feedback of muscle length (*parameter* k_p) and velocity (*parameter* k_v) for each muscle element. Muscle co-contraction was modified using the parameter G_{cc} representing an average baseline muscle activation level, and an additional postural activity Na_{post} was defined to counteract gravity. H_{act} captures muscular activation dynamics. Details can be found in the Appendix.

2.3. Experimental data

We investigated head-neck stabilization by fitting the model to experimental data reported by Forbes et al. (2013b). Twelve subjects (nine men) of 22–26 years were restrained by a five point harness on a rigid seat with a 10° inclined backrest. Subjects were instructed to take on a comfortable upright seating position, maintaining the head comfortably above the torso. Tests were performed with eyes closed (EC) as well as with eyes open (EO). In EC, subjects were blindfolded. In EO, subjects were instructed to maintain visual focus on a stationary target 3 m in front of the platform. During all trials, subjects listened to a science-based radio program to distract them from the stabilization process and minimize voluntary responses. Anterior-posterior pseudorandom multisine (sum of sinusoids) perturbations were applied to the seat using a motion platform. Experiments were performed with four perturbation bandwidths: 0.3–1.2 Hz (B1); 0.3–2.0 Hz (B2); 0.3–4.0 Hz (B4); 0.3–8.0 Hz (B8) all with a root-mean-square (RMS) seat velocity of 0.08 m/s and RMS T1 acceleration of 0.42 (B1); 0.66 (B2); 1.07 (B4); 2.1 (B8) m/s^2. Motion of the seat, T1, and the head were measured using a motion capture system (Qualisys AB, Gothenburg, Sweden), providing head pitch angle and angular velocity $(\theta, \dot{\theta})$, global head forward displacement and velocity $(X_{GH}, \dot{X}_{GH})$, and head forward displacement and velocity relative to T1 $(X_{RH}, \dot{X}_{RH})$. The control parameters were estimated fitting the model to the experimental head translation and rotation using the response averaged over subjects as described in the Appendix.

3. Results

3.1. Model fit to experimental data

The model reproduced the experimentally observed head translation and rotation with good fits in time and frequency domain (Fig. 2) and a variance accounted for (VAF) of 93% averaged over four bandwidths (Table 1) for the eyes closed condition. With eyes open a reasonable fit was obtained with an average VAF of 82% (Fig. 3 and Table 1).

Static stability was evaluated checking head rotation and intervertebral rotations in prolonged simulations without perturbations and with all perturbation conditions. Some parameter variations induced excessive static intervertebral joint motions leading to buckling of the neck and excessive static head rotations in partic-

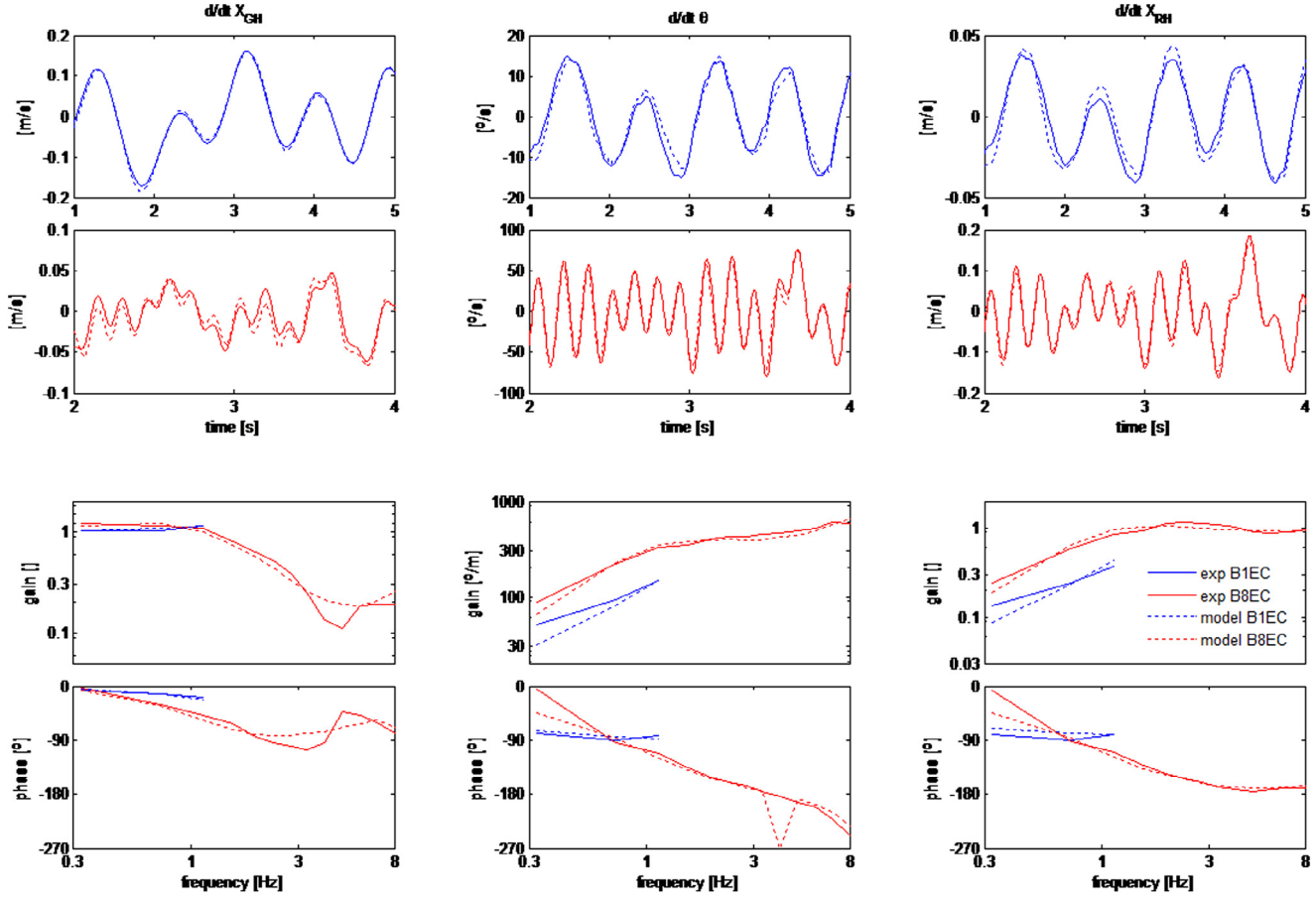

Fig. 2. Model fit with eyes closed. Experimental and modelled kinematic responses in global translational head velocity $\dot{X}_{GH}$, angular head velocity $\dot{\theta}$, and relative translational head velocity $\dot{X}_{RH}$ for the lowest bandwidth (B1-blue) and highest bandwidth (B8-red). Upper plots provide time domain responses, while lower plots provide gain and phase of frequency response functions from T1 translation to head motion.

Table 1
Parameters and variance accounted for (VAF) for the four perturbation bandwidths obtained by fitting the model to experimental data.

Bandwidth	0.3–1.2 Hz (B1)		0.3–2.0 Hz (B2)		0.3–4.0 Hz (B4)		0.3–8.0 Hz (B8)	
Visual feedback	EC	EO	EC	EO	EC	EO	EC	EO
G_{sc} [Nm/(rad/s)]	1.73	2.17	2.11	2.40	0.95	1.22	0.55	1.11
G_{ton} [Nm/rad]	2*	2*	2*	2*	2*	2*	2*	2*
G_{phas} [N/(m/s^2)]	0.87	0.48	3.43	2.46	3.06	2.44	0.87	3.74
k_p [ ]	0.45*	0.45*	0.45*	0.45*	0.56	0.55	0.81	0.65
k_v [1/(1/s)]	0.13	0.12	0.10	0.10	0.10	0.10	0.08	0.07
G_{cc} [%]	1.21	1.08	0.92	0.73	0.84	0.73	0.00	0.00
VAF $\dot{X}_{GH}$	99.5	97.9	96.9	92.6	97.7	94.9	94.9	92.7
VAF $\dot{\theta}$	93.8	78.7	93.4	89.7	97.1	96.0	93.6	81.7
VAF $\dot{X}_{RH}$	92.0	69.2	89.4	74.7	98.0	96.1	97.7	97.3
VAF X_{GH}	99.5	97.3	98.8	94.9	98.8	95.2	97.8	96.3
VAF θ	86.5	48.7	87.0	67.2	91.8	78.4	87.3	83.5
VAF X_{RH}	85.7	38.0	85.2	53.7	92.5	73.4	87.3	81.4
Average VAF	92.8	71.6	91.8	78.8	96.0	89.0	93.1	88.8

* k_p was constrained to be at least 0.45 and G_{ton} was fixed, see text.

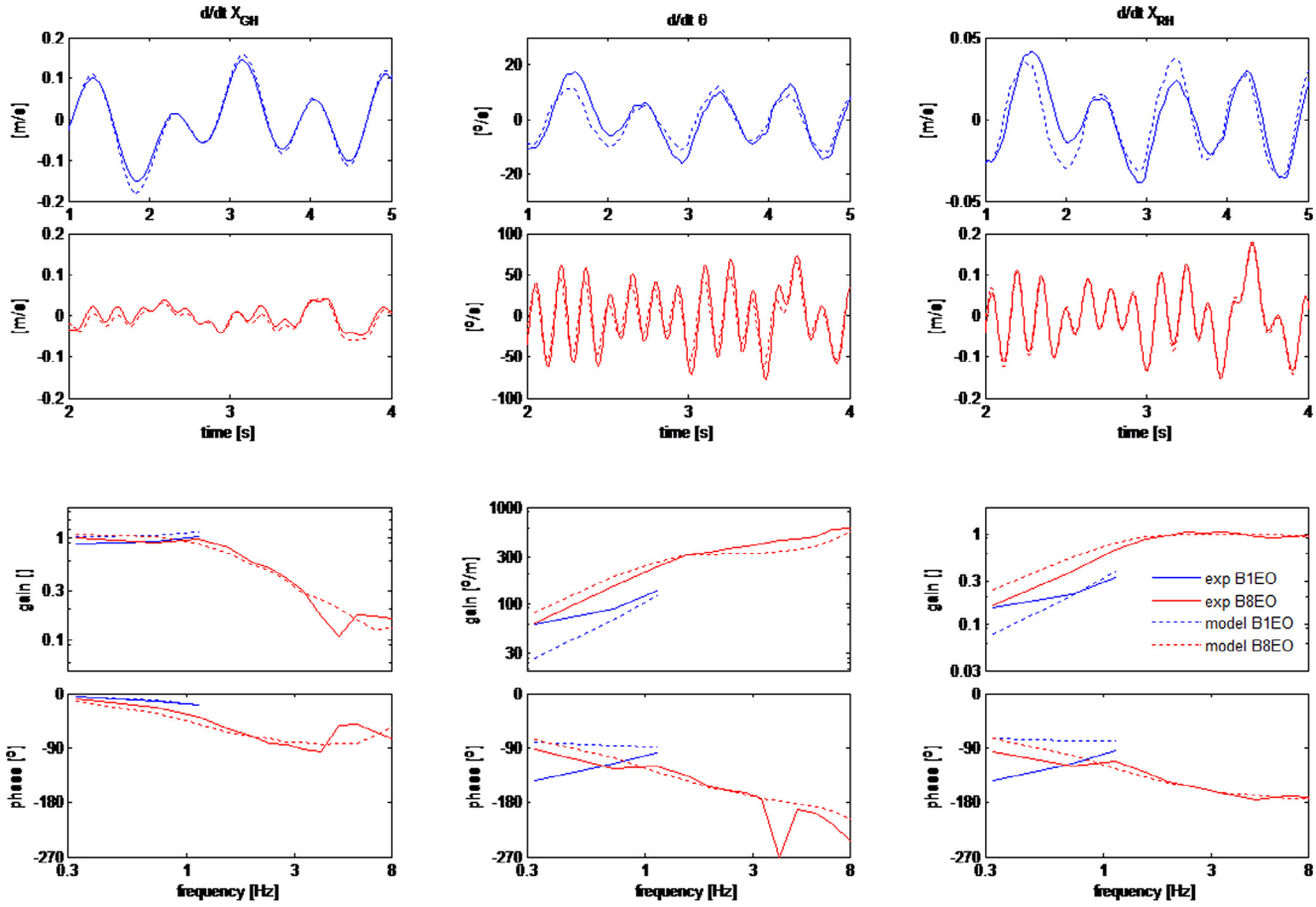

Fig. 3. Model fit with eyes open (further as in Fig. 2).

ular during B1 (see Fig. 4). Apparently in these variations the static feedback gains k_p and G_{ton} and the passive neck stiffness were insufficient to counter the destabilizing effects of gravity. Static stability was achieved by constraining k_p to be greater than 0.45 while G_{ton} was fixed at a value of 2. G_{ton} below 2 induced slow forward or rearward head rotation, in particular with low k_p. A grid search indicated limited effects of G_{ton} on the model fit (Eq. 4 in the Appendix) with optimal G_{ton} below 3 and an adequate model fit with $G_{ton} = 2$.

3.2. Contributions of individual feedback pathways and co-contraction

To examine the influence of VCR, CCR and muscle co-contraction, we simulated different combinations of model parameters varying the best fit parameter sets in Table 1. Omitting the VCR or the CCR strongly affected the static and dynamic response in all conditions. Omitting the VCR resulted in static head rotations up to 13°. Re-optimizing the CCR without VCR provided a reasonable fit (78.5% VAF with $k_p = 0.45$ and $k_v = 0.159$ for B1EC and

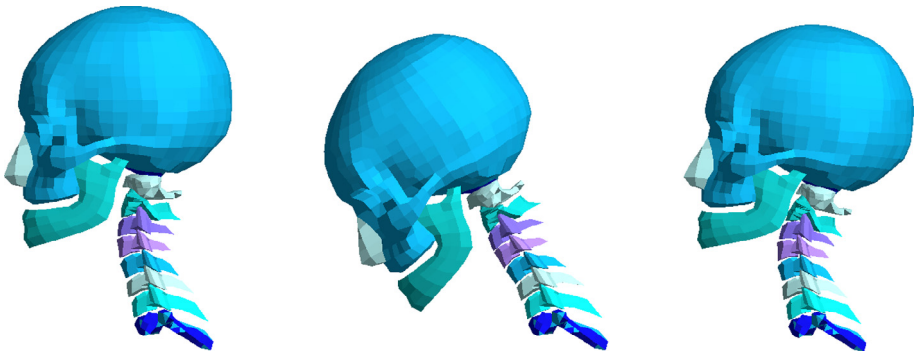

Fig. 4. Static stability illustrated for B1EC. Initial posture (left), forward bending when CCR is disabled (middle), and adequate head position with elevated vestibular feedback (G_{ton} = 12) while CCR is still disabled (right). In the latter condition (right) the spine is locally unstable in the initial posture resulting in rearward buckling of the upper neck segments with joints reaching their range of motion and being stabilized by passive structures.

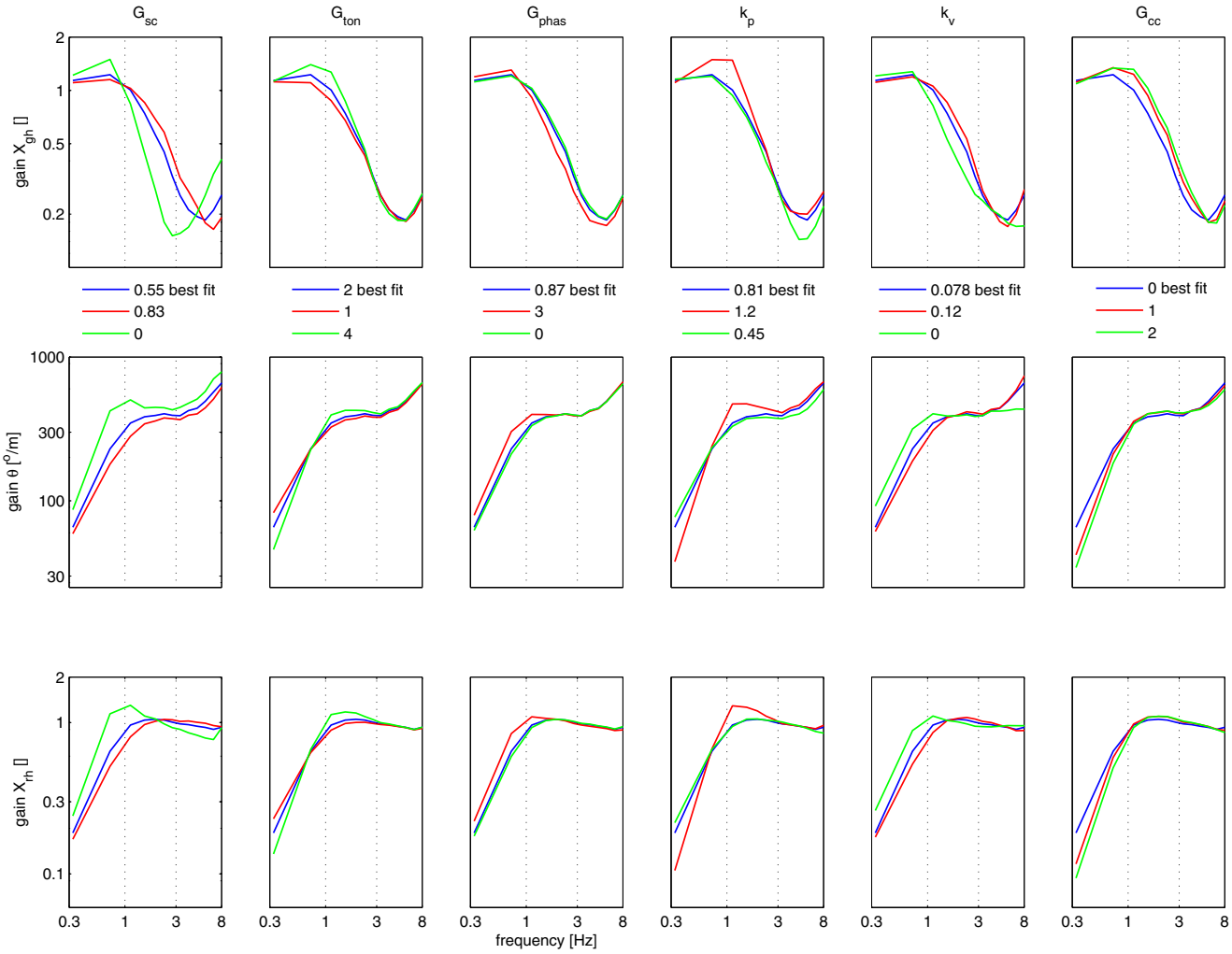

Fig. 5. Variation of the six individual control parameters of the *VCR* (G_{sc}, G_{ton}, G_{phas}), CCR (k_p, k_v) and co-contraction (G_{cc}). The frequency response function from T1 translation to global translational head velocity $\dot{X}_{GH}$ (upper plots), head angular velocity $\dot{\theta}$ (middle plots), and relative translational head velocity $\dot{X}_{RH}$ (lower plots) is depicted for B8EC where the best fit (blue) is equal in all graphs.

85.3% VAF with k_p = 1.06 and k_v = 0.146 for B8EC). Omitting the CCR resulted in neck buckling with static head rotations up to 37° (e.g. Fig. 4). Variation of the six individual control parameters strongly affected the frequency response functions (see Fig. 5 for gain responses in B8EC). As expected, feedback of head angular velocity (G_{sc}) strongly reduced head rotation and this was effective at all tested frequencies (0.3–8 Hz). Hence this feedback is effective beyond the 2–3 Hz range which is often referred to as the resonance frequency of the head-neck system. In addition, G_{sc} reduced head relative translation up to 2 Hz and dampened low frequency oscillations in head rotation and translation. Feedback of head rotation angle (G_{ton}) effectively reduced head rotation up to

0.7 Hz while being counter-effective at higher frequencies. Feedback of head translational acceleration (G_{phas}) had moderate effects reducing head in space translation above 1 Hz at the cost of increased head in space translation below 1 Hz and increased head rotation and relative translation below 2 Hz. As expected, the CCR (k_p and k_v) reduced head rotation and relative translation. CCR length feedback (k_p) was effective up to 0.7 Hz but induced oscillations at 1.1 Hz when raised 50% above the best fit value. CCR velocity feedback (k_v) was effective up to 2 Hz. Co-contraction (G_{cc}) was estimated to be zero for B8 and increasing co-contraction to 1% (similar to the estimate for B1, B2 and B4) led to a relevant reduction of head rotation and head relative displacement up to 1 Hz. Co-contraction increased the head global displacement up to 5 Hz due to a reduced phase lag of the head relative displacement (not shown). It shall be noted that the average muscle activation estimated with the model (~3% for B8 and ~4% for B1, B2, B4) exceeded the co-contraction level. This is partly due to the postural activity Na_{post} counteracting gravity resulting in around 5.5% extensor activation and 2.1% activation averaged over all muscles. Additional muscle activation originates from reflexive stabilization in response to the dynamic perturbations. The activation determines muscular damping through the contractile element (CE) force velocity relationship. We explored this effect by doubling the CE maximum shortening velocity parameter v_{max}, which effectively reduced the CE damping by a factor two. This reduced CE damping had notable effects at all frequencies. Thus, while co-contraction was estimated to be limited or zero, intrinsic muscle damping had a relevant influence on head-neck stabilization.

3.3. Modulation with perturbation bandwidth and vision

The estimated control parameters indicate profound effects of bandwidth with modest effects of vision (Fig. 6 and Table 1). Effects of bandwidth were similar with and without vision (with an exception for G_{phas} at B8 where G_{phas} hardly affected the criterion optimized). The presence of vision led to higher G_{sc} suggesting an increased effort to minimize head rotation. To further analyse effects of bandwidth we also simulated perturbation condition B8 with the parameter sets P1, P2, P4 estimated for the lower bandwidths B1, B2 and B4 and simulated perturbation condition B1 with parameter set P8 estimated for B8 (all with EC). This allowed us to predict effects of low bandwidth control strategies at higher frequencies. The frequency response functions in Fig. 7 show that P1 more effectively reduced head rotation and head relative translation up to 3 Hz (up to a factor 3 at 0.3 Hz) and slightly enlarged head global translation below 1 Hz (17% at 0.7 Hz). P8 reduced global head translation between 1 and 4 Hz with a maximum reduction of 55% at 2.3 Hz. Parameter sets P2 and P4 applied with B8 provided intermediate responses indicating gradual modulation with perturbation bandwidth (not shown). These results indicate a shift towards head-in-space stabilization with higher perturbation bandwidth.

Fig. 7 shows no apparent oscillations in the form of peaks in the frequency response functions. The only slight oscillation occurs at 0.7 Hz where the head global translation gain is 1.26 for P8 at B1 and 1.07 for P1 at B1.

Fig. 7 shows slightly different frequency response functions applying low or high bandwidth perturbations while maintaining the same control parameters (compare continuous and dotted lines of the same colour in Fig. 7). This can be attributed to non-linear model components such as the Hill type muscle model and the activation dynamics.

4. Discussion

We developed a neuromuscular model to investigate contributions of CRR, VCR and muscle co-contraction to head-neck stabilization and modulation of control strategies with perturbation bandwidth and vision.

4.1. Neuromuscular model

The 3D multisegment neck model was developed and validated for impact applications (de Jager, 1996; van der Horst, 2002; Meijer et al., 2013) and was recently enhanced, including validation of muscle moment arms, passive bending stiffness and isometric force generation (de Bruijn et al., 2015). In the current study, we developed a controller for anterior-posterior head-neck stabilization. To our knowledge this is the first multisegment head-neck model including three vestibular feedback loops, length/velocity feedback of individual muscle segments and co-contraction (Fig. 1). Other models include neck muscle synergies grouping muscles as flexors and extensors applying the same activation for all muscles within groups (Brolin et al., 2008; Hedenstierna et al., 2008; Fice et al., 2011; Östh et al., 2012; Dibb et al., 2013; Meijer et al., 2013). We defined muscle synergies generating translational head force, head moments and co-contraction using isometric analyses (de Bruijn et al., 2015). These synergies apply specific activation levels for each muscle segment depending on muscle function, taking into account the moment balance at all joints, enabling separate control of head translation and rotation.

We estimated six neuromuscular control parameters (feedback gains and muscle co-contraction) fitting simulated responses to experiments in which anterior-posterior trunk perturbations were applied to human subjects (Forbes et al., 2013b). The model captured the experimental responses well with some deviations in gain and phase at the lowest frequencies in particular with eyes open. This suggests a need for an additional visual feedback loop, taking into account optokinetic contributions to neck muscle activity. This will best be derived using perturbations with even lower frequencies and manipulating visual information. In the presence of gravity the head-neck system is inherently unstable. Static stability could only be obtained setting minimal values for the two static feedback gains ($k_p > 0.45$ *and* $G_{ton} = 2$) capturing muscle length and vestibular head pitch angle feedback. These were

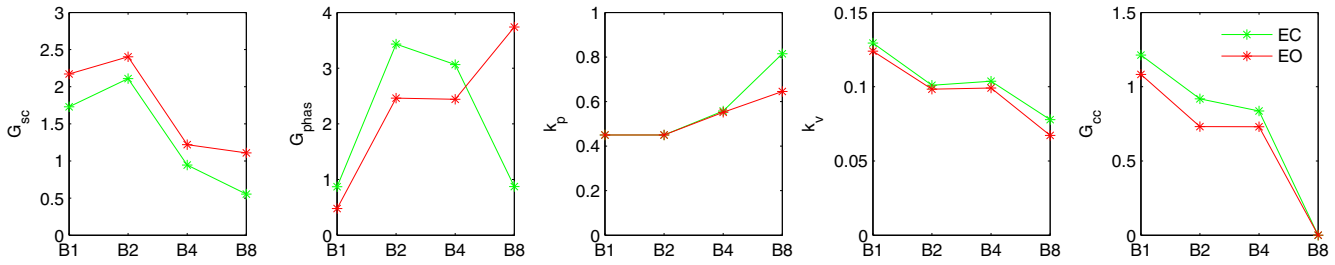

Fig. 6. Effects of bandwidth and vision on the model parameters, estimated for the four perturbation bandwidth conditions (B1–B8) with eyes closed (EC) and eyes open (EO).

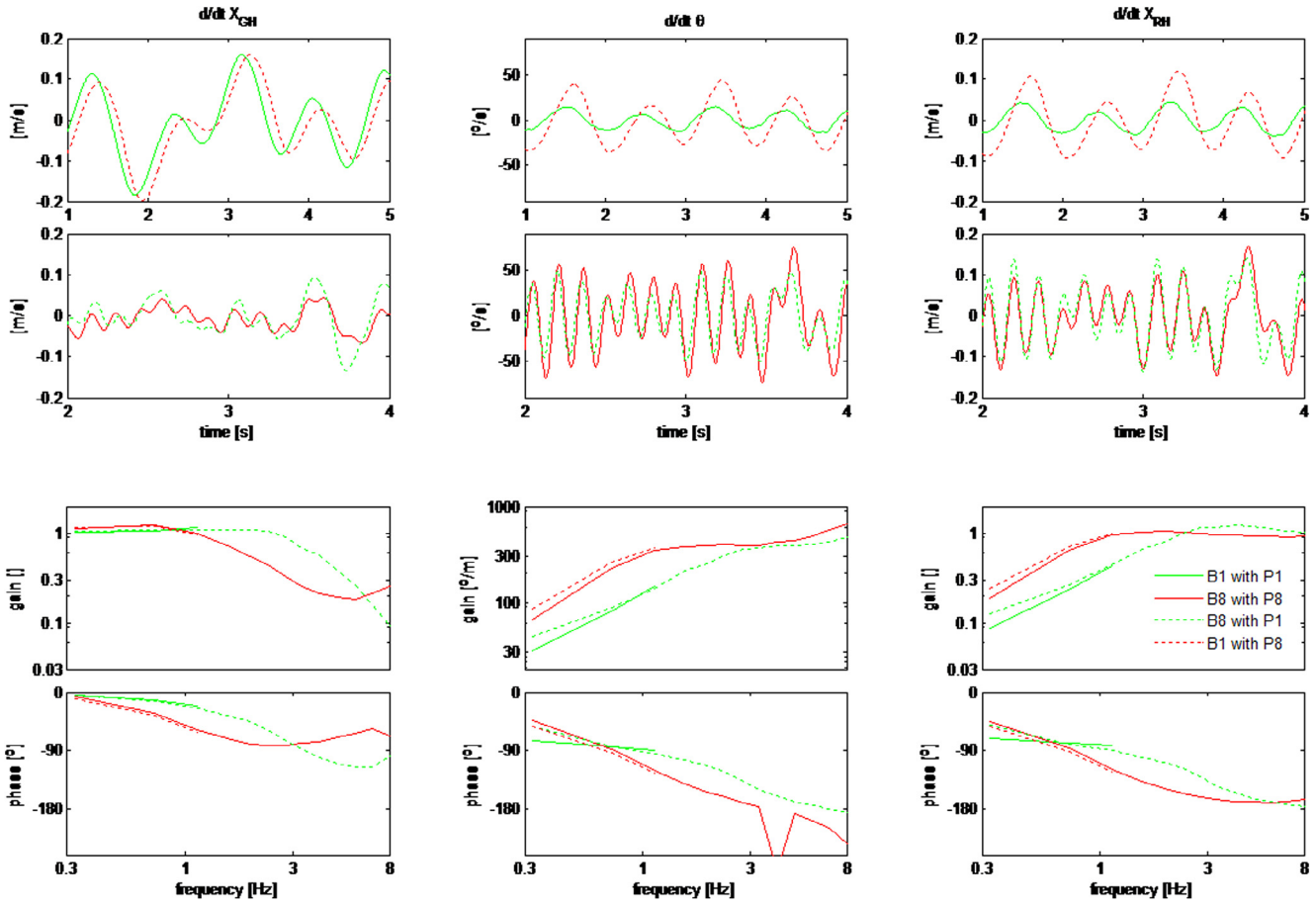

Fig. 7. Effects of bandwidth; parameter set (P1) estimated for the lowest bandwidth (B1) and parameter set P8 estimated for the highest bandwidth (B8) with eyes closed, have been used to simulate both conditions (B1&B8).

partially interchangeable; selecting higher k_p values a lower G_{ton} could still stabilize head rotation, but k_p was essential to stabilize the intervertebral joints, and G_{ton} was most effective to minimize static head rotation. A more precise estimation of these parameters may be possible using experiments with low frequency perturbations, where the distinct role of k_p (head-on-trunk) and G_{ton} (head-in-space) could be revealed using independent torso translation and rotation perturbations. The other control parameters (G_{sc}, G_{phas}, k_v, G_{cc}) could well be estimated by fitting head translation and rotation kinematics, where Fig. 5 shows that these parameters have markedly different effects. Here it is noted that the model contains many parameters characterising discs, facet joints and ligaments. The resulting intervertebral bending stiffness has been validated by de Bruijn et al. (2015), but dynamic validation of the passive spine is recommended. With further validation, the model can be of value in the medical field for research, diagnosis and treatment of neck disorders and in fields such as vehicle comfort and impact biomechanics.

4.2. Contributions of individual feedback pathways and co-contraction

The VCR contributed to head-in-space stabilization through a strong reduction of head rotation and a moderate reduction of head global translation. The CCR contributed to head-on-trunk stabilization with a substantial reduction of head rotation and head relative translation. These results support hypothesis 1 where contributions vary in magnitude and frequency range. The VCR reduced head rotation with a substantial contribution of semicircular feedback (G_{sc}) at all tested frequencies (Fig. 5) and with tonic otolith feedback (G_{ton}) contributing to static stability. The VCR reduced head-in-space translation through phasic otolith feedback (G_{phas}) (Fig. 5). CCR velocity feedback (k_v) reduced head rotation and relative translation up to 2 Hz while length feedback (k_p) was effective up to 0.7 Hz (Fig. 5). These results are in line with modelling studies reporting a similar magnitude of VCR and CCR contributions to control head rotation in the sagittal plane (Peng, 1996; Peng et al., 1997). We are not aware of any other model controlling head-in-space translation using otolith feedback. In our model this feedback was moderately effective above 1 Hz while at lower frequencies both experiment and model show head-on-trunk stabilization. This aligns with the selected otolith transfer function, which has a low sensitivity below 1 Hz (Fig. 9 right). Further exploration of otolith feedback contributions to head translation control could thus focus on perturbations above 1 Hz.

The CCR proved essential to stabilize the individual intervertebral joints and prevent neck buckling, which confirms hypothesis 2. Without CCR, static stability could not be achieved resulting in excessive static flexion or extension of the individual neck joints and the entire neck (Fig. 4). A model without VCR could be stabilized provided CCR gains were adapted, which is also seen in vestibular loss patients where "there are no dramatic differences between patients and controls" in conditions similar to the current study (Keshner, 2003).

The level of co-contraction (G_{cc}) was estimated to be around 1% for bandwidths B1, B2, B4 and zero with the highest bandwidth B8. The 1% co-contraction contributed to head-on-trunk stabilization up to 1 Hz (Fig. 5) but was not essential for dynamic and static stabilization. This supports hypothesis 3, and highlights a minor

contribution of co-contraction in natural head-neck stabilization conditions. However, additional postural activation to counteract gravity and reflexive activation in response to the dynamic perturbations resulted in average muscle activation levels of 3–4% inducing relevant intrinsic muscle resistance through the contractile element (CE) force velocity relationship. Here it shall be noted that Keshner (2000) found that both younger (20–40 years) and older (65–88 year) subjects showed effective co-contraction when asked to stiffen their necks, while the older subjects also showed effective co-contraction with mental arithmetic and relax tasks.

4.3. Modulation with perturbation bandwidth and vision

The estimated control parameters indicate profound effects of bandwidth with modest effects of vision (Fig. 6 and Table 1). Effects of bandwidth were similar with and without vision. Vision led to increased semicircular feedback (G_{sc}) indicating elevated efforts to minimize head rotation. This concurs with the notion that vestibular and visual senses integrate to improve the perception of motion (Angelaki et al., 2011). The current model captured this in a simplified manner as an increased usage of vestibular feedback. Other parameters also suggest a shift towards head-in-space stabilization with vision, but effects were small for k_v and G_{cc} and present only at the highest bandwidth for G_{phas} and k_p.

Studies on the extremities indicate that feedback gains are reduced with increasing perturbation bandwidths to prevent feedback induced oscillations at the system's natural frequency (Kearney et al., 1997; Mugge et al., 2010). In our experimental study (Forbes et al., 2013b), we hypothesized a similar feedback gain reduction in the neck with perturbation bandwidths exceeding the natural frequency. The parameter estimates from our model (Fig. 6) indeed showed reduced feedback gains G_{sc} and k_v with higher bandwidths, but this is accompanied with increased gains G_{phas} and k_p. The model allowed us to predict the effects of control strategies identified for high bandwidth conditions with lower bandwidth perturbations (and vice versa). As illustrated in Fig. 7, the low bandwidth control strategy P1 does not induce apparent oscillations when simulated with the highest bandwidth perturbation (i.e. B8 with P1). Therefore we conclude that attenuation of oscillations does not explain the observed modulation of neck stabilization strategies with changes in perturbation bandwidth.

The experimental data up to 1.2 Hz (see Figs. 2 and 3) motivated hypothesis 4: *The presence of higher frequencies in the perturbations will induce a shift from head-on-trunk to head-in-space stabilization.* Our neuromuscular model supported hypothesis 4 also for frequencies above 1.2 Hz. As illustrated in Fig. 7, the control strategy employed at the lowest bandwidth more effectively reduced head rotation and head relative displacement up to 3 Hz as compared to the high bandwidth control strategy. In contrast, the control strategy employed at the highest bandwidth reduced head global translation between 1 and 4 Hz, an outcome that could not be identified experimentally. In terms of head translation, this indicates a shift from head-on-trunk stabilization at the lowest bandwidth to head-in-space stabilization at the highest bandwidth. Our parameter estimates suggest that this was realized by reduced muscle velocity feedback (k_v) and co-contraction (G_{cc}), combined with increased head translational acceleration feedback (G_{ton}). In terms of head rotation, the experiment did not discriminate between head-in-space and head-on-trunk stabilization because the trunk was perturbed in translation only. Experiments inducing trunk rotation could provide further insight in the interacting and partially opposing VCR and CCR contributions to control head rotation. The control strategy with the highest perturbation bandwidth led to an increased head rotation which may not seem beneficial, but apparently helps to reduce head global translation from 1 to 4 Hz (Fig. 7). This interaction is also apparent in the effect of G_{sc} on X_{gh} in Fig. 5. Summarizing results for translation and rotation, we observe a shift in control strategy from minimizing head-on-trunk rotation and translation during low bandwidth perturbations to minimizing head-in-space translation during high bandwidth perturbations. This modulation of control may well be beneficial in terms of comfort, limiting the transfer of 1–4 Hz horizontal seat motions to the head, where comfort standards for whole body vibration attribute considerable weight to these frequencies (ISO-2631-1 1997).

Conflicts of interest statement

The authors declare that no conflict of interest were associated with the present study.

Acknowledgements

This research was supported by the Dutch Technology Foundation STW, which is part of the Netherlands Organization for Scientific Research (NWO) and partly funded by the Ministry of Economic Affairs, Agriculture and Innovation (www.neurosipe.nl project 10736: torticollis). We acknowledge the advice of M. Jamali and K. Cullen for the implementation of vestibular functions, and TNO and TASS International for supporting the model implementation.

Appendix A. Model equations and parameter estimation

Supplementary data associated with this article can be found, in the online version, at http://dx.doi.org/10.1016/j.jbiomech.2017.05.005.

References

Almeida, J., Fraga, F., Silva, M., Silva-Carvalho, L., 2009. Feedback control of the head-neck complex for nonimpact scenarios using multibody dynamics. Multibody Sys.Dyn. 21, 395–416. http://dx.doi.org/10.1007/s11044-009-9148-4.

Angelaki, D.E., Gu, Y., Deangelis, G.C., 2011. Visual and vestibular cue integration for heading perception in extrastriate visual cortex. J. Physiol. 589, 825–833. http://dx.doi.org/10.1113/jphysiol.2010.194720.

Borst, J., Forbes, P.A., Happee, R., Veeger, H.E.J., 2011. Muscle parameters for musculoskeletal modelling of the human neck. Clin. Biomech. (Bristol, Avon) 26, 343–351. http://dx.doi.org/10.1016/j.clinbiomech.2010.11.019. S0268-0033(10)00313-X [pii].

Brolin, K., Hedenstierna, S., Halldin, P., Bass, C., Alem, N., 2008. The importance of muscle tension on the outcome of impacts with a major vertical component. Int. J. Crashworthiness 13, 487–498. http://dx.doi.org/10.1080/13588260802215510.

Chancey, V.C., Nightingale, R.W., Van Ee, C.A., Knaub, K.E., Myers, B.S., 2003. Improved estimation of human neck tensile tolerance: reducing the range of reported tolerance using anthropometrically correct muscles and optimized physiologic initial conditions. Stapp Car Crash J. 47, 135–153. doi: 2003-22-0008 [pii].

Cullen, K.E., 2012. The vestibular system: multimodal integration and encoding of self-motion for motor control. Trends Neurosci. 35, 185–196. http://dx.doi.org/10.1016/j.tins.2011.12.001.

de Bruijn, E., van der Helm, F.C.T., Happee, R., 2015. Analysis of isometric cervical strength with a nonlinear musculoskeletal model with 48 degrees of freedom. Multibody Sys.Dyn. 36, 339–362. http://dx.doi.org/10.1007/s11044-015-9461-z.

de Jager, M.K.J., 1996. Mathematical Head-Neck Models for Acceleration Impacts. PhD thesis. In. University of Eindhoven, p. 143.

de Vlugt, E., Schouten, A.C., van der Helm, F.C.T., 2006. Quantification of intrinsic and reflexive properties during multijoint arm posture. J. Neurosci. Methods 155, 328–349. http://dx.doi.org/10.1016/j.jneumeth.2006.01.022.

Dibb, A.T., Cox, C.A., Nightingale, R.W., et al., 2013. Importance of muscle activations for biofidelic pediatric neck response in computational models. Traffic Injury Prevent. 14, S116–S127. http://dx.doi.org/10.1080/15389588.2013.806795.

Fard, M.A., Ishihara, T., Inooka, H., 2003. Dynamics of the head-neck complex in response to the trunk horizontal vibration: modeling and identification. J. Biomech. Eng. 125, 533–539.

Fard, M.A., Ishihara, T., Inooka, H., 2004. Identification of the head-neck complex in response to trunk horizontal vibration. Biol. Cybern. 90, 418–426. http://dx.doi.org/10.1007/s00422-004-0489-z.

Fice, J.B., Cronin, D.S., Panzer, M.B., 2011. Cervical spine model to predict capsular ligament response in rear impact. Ann. Biomed. Eng. 39, 2152–2162. http://dx.doi.org/10.1007/s10439-011-0315-4.

Forbes, P.A., Dakin, C.J., Vardy, A.N., Happee, R., Siegmund, G.P., Schouten, A.C., Blouin, J.S., 2013a. Frequency response of vestibular reflexes in neck, back, and lower limb muscles. J. Neurophysiol. 110, 1869–1881. http://dx.doi.org/10.1152/jn.00196.2013.

Forbes, P.A., de Bruijn, E., Schouten, A.C., van der Helm, F.C.T., Happee, R., 2013b. Dependency of human neck reflex responses on the bandwidth of pseudorandom anterior-posterior torso perturbations. Exp. Brain Res. 226, 1–14. http://dx.doi.org/10.1007/s00221-012-3388-x.

Gillies, G.T., Broaddus, W.C., Stenger, J.M., Taylor, A.G., 1998. A biomechanical model of the craniomandibular complex and cervical spine based on the inverted pendulum. J. Med. Eng. Technol. 22, 263–269.

Goldberg, J., Peterson, B.W., 1986. Reflex and mechanical contributions to head stabilization in alert cats. J. Neurophysiol. 56, 857–875.

Goldberg, J.M., Cullen, K.E., 2011. Vestibular control of the head: possible functions of the vestibulocollic reflex. Exp. Brain Res. 210, 331–345. http://dx.doi.org/10.1007/s00221-011-2611-5.

Hedenstierna, S., 2008. 3D Finite Element Modeling of Cervical Musculature and its Effect on Neck Injury Prevention. In. KTH, PhD thesis, Stockholm, pp. vii, 60.

Hedenstierna, S., Halldin, P., Brolin, K., 2008. Evaluation of a combination of continuum and truss finite elements in a model of passive and active muscle tissue. Comp. Methods Biomech. Biomed. Eng. 11, 627–639. http://dx.doi.org/10.1080/17474230802312516.

ISO-2631-1., 1997. Mechanical Vibration and Shock: Evaluation of Human Exposure to Whole-Body Vibration.

Kearney, R.E., Stein, R.B., Parameswaran, L., 1997. Identification of intrinsic and reflex contributions to human ankle stiffness dynamics. IEEE Trans. Biomed. Eng. 44, 493–504.

Keshner, E.A., 2000. Modulating active stiffness affects head stabilizing strategies in young and elderly adults during trunk rotations in the vertical plane. Gait Posture 11, 1–11.

Keshner, E.A., 2003. Head-trunk coordination during linear anterior-posterior translations. J. Neurophysiol. 89, 1891–1901. http://dx.doi.org/10.1152/jn.00836.2001.

Keshner, E.A., 2009. Vestibulocollic and cervicocollic control. In: Binder, M.D., Jirokawa, N., Windhorst, U. (Eds.), Encyclopedia of Neuroscience. Springer-Verlag, Berlin, Heidelberg, pp. 4222–4224.

Keshner, E.A., Hain, T.C., Chen, K.J., 1999. Predicting control mechanisms for human head stabilization by altering the passive mechanics. J. Vestib. Res. 9, 423–434.

Liang, C.C., Chiang, C.F., 2008. Modeling of a seated human body exposed to vertical vibrations in various automotive postures. Ind. Health 46, 125–137. http://dx.doi.org/10.2486/indhealth.46.125.

Meijer, R., Broos, J., Elrofai, H., de Bruijn, E., Forbes, P.A., Happee, R., 2013. Modelling of bracing in a multi-body active human model. In: IRCOBI, vol. IRC-13-67, Gothenburg, Sweden, pp. 576-587.

Mirbagheri, M.M., Barbeau, H., Kearney, R.E., 2000. Intrinsic and reflex contributions to human ankle stiffness: variation with activation level and position. Exp. Brain Res. 135, 423–436.

Mugge, W., Abbink, D.A., Schouten, A.C., Dewald, J.P.A., van der Helm, F.C.T., 2010. A rigorous model of reflex function indicates that position and force feedback are flexibly tuned to position and force tasks. Exp. Brain Res. 200, 325–340. http://dx.doi.org/10.1007/s00221-009-1985-0.

Östh, J., Brolin, K., Carlsson, S., Wismans, J., Davidsson, J., 2012. The occupant response to autonomous braking: a modeling approach that accounts for active musculature. Traffic Inj Prev 13, 265–277. http://dx.doi.org/10.1080/15389588.2011.649437.

Östh, J., Brolin, K., Svensson, M.Y., Linder, A., 2016. A female ligamentous cervical spine finite element model validated for physiological loads. J. Biomech. Eng. 138. http://dx.doi.org/10.1115/1.4032966.

Paddan, G.S., Griffin, M.J., 1998. A review of the transmission of translational seat vibration to the head. J. Sound Vib. 215, 863–882.

Panjabi, M.M., Crisco, J.J., Vasavada, A., Oda, T., Cholewicki, J., Nibu, K., Shin, E., 2001. Mechanical properties of the human cervical spine as shown by three-dimensional load-displacement curves. Spine 26, 2692–2700. http://dx.doi.org/10.1097/00007632-200112150-00012.

Peng, G.C., Hain, T.C., Peterson, B.W., 1999. Predicting vestibular, proprioceptive, and biomechanical control strategies in normal and pathological head movements. IEEE Trans. Biomed. Eng. 46, 1269–1280. http://dx.doi.org/10.1109/10.797986.

Peng, G.C.Y., 1996. Dynamics and control of head, neck and eye stabilization: neuromechanical and experimental models. In: vol. PhD Thesis. Northwestern University.

Peng, G.C.Y., Hain, T.C., Peterson, B.W., 1997. How is the head held up? Modeling mechanisms for head stability in the sagittal plane. In: Boom, H., Robinson, C., Rutten, W., Neuman, M., Wijkstra, H. (Eds.), Proceedings of the 18th Annual International Conference of the IEEE Engineering in Medicine and Biology Society, vol. 18, Pts 1–5, vol. 18, pp. 627–628.

Pintar, F.A., 1986. The biomechanics of spinal elements (ligaments, vertebral body, disc). In: Marquette University, PhD thesis.

Rahmatalla, S., Liu, Y., 2012. An active head-neck model in whole-body vibration: vibration magnitude and softening. J. Biomech. 45, 925–930. http://dx.doi.org/10.1016/j.jbiomech.2012.01.022.

Reynolds, J.S., Blum, D., Gdowski, G.T., 2008. Reweighting sensory signals to maintain head stability: adaptive properties of the cervicocollic reflex. J. Neurophysiol. 99, 3123–3135. http://dx.doi.org/10.1152/jn.00793.2007.

Stemper, B.D., Yoganandan, N., Pintar, F.A., 2004. Validation of a head-neck computer model for whiplash simulation. Med. Biol. Eng. Compu. 42, 333–338. http://dx.doi.org/10.1007/bf02344708.

van der Horst, M.J., 2002. Human head and neck response in frontal, lateral, and impact loading. PhD thesis. In: Technical University of Eindhoven, Eindhoven, p. 218.

van Drunen, P., Maaswinkel, E., van der Helm, F.C.T., van Dieën, J.H., Happee, R., 2013. Identifying intrinsic and reflexive contributions to low-back stabilization. J. Biomech. 46, 1440–1446. http://dx.doi.org/10.1016/j.jbiomech.2013.03.007.

van Ee, C.A., Nightingale, R.W., Camacho, D.L., Chancey, V.C., Knaub, K.E., Sun, E.A., Myers, B.S., 2000. Tensile properties of the human muscular and ligamentous cervical spine. Stapp Car Crash J. 44, 85–102. doi: 2000-01-SC07 [pii].

Wang, Y., Rahmatalla, S., 2013. Human head-neck models in whole-body vibration: effect of posture. J. Biomech. 46, 702–710. http://dx.doi.org/10.1016/j.jbiomech.2012.11.037.

Wittek, A., Kajzer, J., Haug, E., 2000. Hill-type muscle model for analysis of mechanical effect of muscle tension on the human body response in a car collision using an explicit finite element code. Jsme Int. J. Ser. Solid Mech. Mater. Eng. 43, 8–18.

Yoganandan, N., Pintar, F.A., Cusick, J.F., 2002. Biomechanical analyses of whiplash injuries using an experimental model. Accid. Anal. Prev. 34, 663–671. http://dx.doi.org/10.1016/s0001-4575(01)00066-5.

Yoganandan, N., Pintar, F., Kumaresan, S., Elhagediab, A., 1998. Biomechanical assessment of human cervical spine ligaments. SAE Tech. Pap., 983159 http://dx.doi.org/10.4271/983159.